

See discussions, stats, and author profiles for this publication at: <https://www.researchgate.net/publication/13395114>

The Conserved Arginine in Rho-GTPase-Activating Protein Is Essential for Efficient Catalysis but Not for Complex Formation with Rho·GDP and Aluminum Fluoride †

ARTICLE *in* BIOCHEMISTRY · FEBRUARY 1999

Impact Factor: 3.02 · DOI: 10.1021/bi9821770 · Source: PubMed

CITATIONS

69

READS

16

3 AUTHORS, INCLUDING:



[Debbie L. Cunningham](#)

University of Birmingham

16 PUBLICATIONS 393 CITATIONS

SEE PROFILE



[Peter Lowe](#)

74 PUBLICATIONS 1,989 CITATIONS

SEE PROFILE

The Conserved Arginine in Rho-GTPase-Activating Protein Is Essential for Efficient Catalysis but Not for Complex Formation with Rho•GDP and Aluminum Fluoride[†]

Debbie L. Graham,^{‡,§} John F. Eccleston,[‡] and Peter N. Lowe^{*,§}

Division of Physical Biochemistry, National Institute of Medical Research, The Ridgeway, Mill Hill, London NW7 1AA, and GlaxoWellcome Medicines Research Centre, Gunnels Wood Road, Stevenage, Herts SG1 2NY, U.K.

Received September 10, 1998

ABSTRACT: The Rho family of small GTP-binding proteins are downregulated by an intrinsic GTPase, which is enhanced by GTPase-activating proteins (GAPs). RhoGAPs contain a single conserved arginine residue that has been proposed to be involved in catalysis. Here, the role of this arginine has been elucidated by mutagenesis followed by determination of catalytic and equilibrium binding constants using single-turnover kinetics, isothermal titration calorimetry, and scintillation proximity assays. The turnover numbers for wild-type, R282A, and R282K RhoGAPs were 5.4, 0.023, and 0.010 s⁻¹, respectively. Thus, the function of this arginine could not be replaced by lysine or alanine. Nevertheless, the R282A mutation had a minimal effect on the binding affinity of RhoGAP for either Rho•GTP or Rho•GMPPNP, which confirms the importance of the arginine residue for catalysis as opposed to formation of the protein–protein complex. The R282A mutant RhoGAP still increased the hydrolysis rate of Rho•GTP by 160-fold, whereas the wild-type enzyme increased it by 38000-fold. We conclude that this arginine contributes half of the total reduction of activation energy of catalysis. In the presence of aluminum fluoride, the R282A mutant RhoGAP binds almost as well as the wild type to Rho•GDP, demonstrating that the conserved arginine is not required for this interaction. The affinity of wild-type RhoGAP for the triphosphate form of Rho is similar to that for Rho•GDP with aluminum fluoride. These last two observations show that this complex is not associated with the free energy changes expected for the transition state, although the Rho•GDP•AlF₄⁻•RhoGAP complex might well be a close structural approximation.

Rho, Cdc42, and Rac are members of the Rho family of small GTP-binding proteins that control key cellular processes, including actin organization, cytokinesis, transcription, secretion, and endocytosis (1, 2). Rho family proteins cycle between an inactive GDP-bound form and an active GTP-bound form. The GTP form binds protein effectors which transmit downstream signals. They are downregulated by GTPase-activating proteins (GAPs¹), which stimulate their intrinsic GTPase activity. The RhoGAP family proteins, including bcr, n-chimaerin, p190, and RhoGAP, all contain a homologous catalytic domain (3). Within this domain is a single conserved arginine residue (4); in the case of RhoGAP, it is Arg-282 [identical to Arg-85 of the crystallized RhoGAP domain (5, 6)]. X-ray crystallography studies of the complex between RhoGAP, Rho•GDP, and AlF₄⁻, which was proposed to be an analogue of the transition state, have shown

that this residue is placed directly into the active site of Rho, suggesting a direct role for Arg-282 in the hydrolysis of GTP by RhoGAP (6). This role is similar to that proposed for invariant arginines in Ras-GAPs (7–10) and in G_α (11, 12).

Although experimental data supporting the role of this conserved arginine in catalysis by RhoGAPs have recently been published (13–18), hitherto the effect of mutagenesis of this residue on the turnover number (*k*_{cat}) has not been available. Therefore, we have measured the effect of mutation to either alanine or lysine on the *k*_{cat} for enhancement of Rho-GTPase and on the affinity for binding to substrate. These data showed that the basic center of arginine is indeed essential for efficient catalysis and cannot be replaced by that of lysine. We also examined the properties of the AlF_x-mediated Rho•GDP•RhoGAP complex and the role of the conserved arginine in its formation. Perhaps unexpectedly, on the basis of existing literature, the replacement with alanine did not affect formation of a complex with Rho•GDP and AlF_x. We show that the Rho•GDP•AlF_x•RhoGAP complex is not associated with the free energy changes expected for the transition state, although it might well be a close structural approximation.

EXPERIMENTAL PROCEDURES

Proteins and Nucleotide Complexes. Plasmids expressing GST–RhoGAP or GST–RhoA [the latter containing a point

[†] This work was supported by the Medical Research Council, United Kingdom.

^{*} To whom correspondence should be addressed. Telephone: +44 (0)1438 763867. Fax: +44 (0)1438 764818. E-mail: PL44712@ggr.co.uk.

[‡] National Institute of Medical Research.

[§] GlaxoWellcome Medicines Research Centre.

¹ Abbreviations: SPA, scintillation proximity assay; ITC, isothermal titration calorimetry; DTT, dithiothreitol; GAP, GTPase-activating protein; AlF_x, aluminum fluoride (exact chemical species not defined); mant, 2'(3')-O-N-methylanthraniloyl; GMPPNP, 5'-guanylylimido diphosphate.

mutation (F25N) to improve stability (19)] were generous gifts from A. Hall. Arg-282 of GST-RhoGAP (C-terminal fragment residues 198–439, numbered from the first residue of full-length p50 RhoGAP) (4) was mutated to alanine and lysine using the Stratagene QuikChange mutagenesis kit. The plasmids containing GST-RhoGAP (wild-type or mutant) and GST-Rho were transformed into *Escherichia coli* DH5 α and BL21, respectively. Proteins were expressed as GST fusions and were purified with and without the GST tag on glutathione agarose columns as previously described (20). Proteins were finally dialyzed against 20 mM Tris-HCl (pH 7.5), 2 mM MgCl $_2$, and 1 mM DTT. All proteins had the anticipated M_r when they were analyzed by electrospray mass spectrometry. Protein concentrations were calculated from the A_{280} using extinction coefficients of 14 420 M $^{-1}$ cm $^{-1}$ for RhoGAP and 26 430 M $^{-1}$ cm $^{-1}$ for Rho, calculated from the extinction coefficients of Tyr and Trp (21) and that of GTP (7950 M $^{-1}$ cm $^{-1}$). Rho- $^{[3]}\text{H}$ GTP, Q61L Rac- $^{[3]}\text{H}$ GTP, and Q63L Rho- $^{[3]}\text{H}$ GTP were prepared as described for Q61L Ras- $^{[3]}\text{H}$ GTP (22). Rho-GMPPNP was prepared as described for Rac/Cdc42-GMPPNP (23). Rho-mant nucleotide complexes were prepared as described previously (20, 24).

Measurements of GTPase Activity. All experiments were carried out in 20 mM Tris-HCl (pH 7.5), 2 mM MgCl $_2$, and 1 mM DTT at 20 °C. For measurements of intrinsic GTPase activity, or mutant RhoGAP-catalyzed GTPase activity, 0.2 μM Rho- $^{[3]}\text{H}$ GTP was incubated with 0–30 μM RhoGAP. At intervals, 100 μL samples were mixed with 50 μL of 10% perchloric acid and then adjusted to pH 4 by addition of 17 μL of 4 M sodium acetate. For measurements of wild-type RhoGAP-catalyzed GTPase activity, Rho- $^{[3]}\text{H}$ GTP (0.2 μM) was mixed with wild-type RhoGAP in a Hi-Tech Rapid Quench Flow system using perchloric acid to quench, and then samples were removed and adjusted to pH 4 with sodium acetate. Samples were analyzed by anion exchange HPLC with radiochemical detection (Berthold) using a Partisphere SAX column (Whatman) with a mobile phase of 0.6 M NH $_4$ H $_2$ PO $_4$ (pH 4). The decrease in the amount of $^{[3]}\text{H}$ GTP was fitted to a single-exponential decay curve to give a pseudo-first-order rate constant for GTP hydrolysis. Data on the effect of concentration of RhoGAP on this rate constant were analyzed as described in ref 10 to give k_{cat} and K_m .

Fluorescence Measurements. Fluorescence anisotropy titrations of RhoGAP into Rho-mantGDP were performed essentially as described previously (20), except that the experiments were carried out at 20 °C in 20 mM Tris-HCl (pH 7.5), 2 mM MgCl $_2$, 1 mM DTT, 110 μM AlCl $_3$, and 20 mM NaF.

Isothermal Titration Calorimetry (ITC). ITC was performed in a Microcal MCS calorimeter (25). Rho-GMPPNP or Rho-GDP (180 μM ; preliminary 2 μL injection followed by up to 25 injections of 10 μL) was injected into 15 μM RhoGAP or buffer (for control) at 20 °C. For AIF $_x$ experiments, 110 μM AlCl $_3$ and 20 mM NaF were present in all solutions. The heat output from the control titration was subtracted using MicroCal Origin software, and the resultant data were fitted to a binding isotherm describing binding at a single site (25) to estimate K_d , ΔH , and stoichiometry (n).

Scintillation Proximity Assay (SPA). Scintillation proximity assays were similar to those described in ref 23. Affinities

of wild-type Rho-GDP and Rho-GMPPNP for RhoGAPs were measured using a competition assay consisting of 1.25 mg of Protein A SPA PVT beads (Amersham catalog no. RPNQ 0019), 4.5 μg of anti-GST antibody (Molecular Probes), 0.025 μM Q61L Rac- $^{[3]}\text{H}$ GTP, 0.02 μM GST-RhoGAP (wild-type or mutant), 20 mM Tris-HCl (pH 7.5), 2 mM MgCl $_2$, 1 mM DTT, 0.2 mg/mL BSA, and competing protein (up to 16 μM) in a final volume of 200 μL . Experiments with AIF $_x$ included 110 μM AlCl $_3$ and 20 mM NaF. Apparent K_d s for competing proteins were determined as described in ref 23, taking the K_d for Q61L Rac- $^{[3]}\text{H}$ GTP binding to wild-type and R282A GST-RhoGAPs to be 0.2 and 0.06 μM , respectively. The affinities of Q61L Rac- $^{[3]}\text{H}$ GTP and of Q63L Rho- $^{[3]}\text{H}$ GTP were measured by direct titration SPAs with 0.02 μM GST-RhoGAP (wild-type or mutant) as described in ref 23.

RESULTS

Catalytic Activity of Wild-Type, R282A, and R282K RhoGAP. Single-turnover kinetic experiments (9, 10, 20), in which the GTP hydrolysis rate was measured under conditions where RhoGAP (the enzyme) is in molar excess over Rho- $^{[3]}\text{H}$ GTP (the substrate), were used to determine the kinetic parameters for activation of Rho-GTPase by wild-type, R282A, and R282K RhoGAPs. An advantage of this procedure over steady-state kinetic measurements is that the maximally activated rate constant (k_{cat}) is independent of the concentration of GAP (20). An estimate of K_m can also be obtained. Although it was technically more difficult, we decided to directly measure cleavage of GTP itself rather than monitoring fluorescence changes of mant nucleotides as has previously been done in such experiments (9, 10, 20, 26). This was done because, in specific circumstances, mant nucleotides were not perfect analogues of native nucleotides (see below) and also to avoid any assumptions in relating rates of fluorescence changes to cleavage rates.

Time courses of hydrolysis at near-saturating, fixed concentrations of wild-type and mutant RhoGAPs (panel A) and the effect of concentration of RhoGAP on the pseudo-first-order rate constant for hydrolysis (panels B and C) are shown in Figure 1. k_{cat} was found to be 5.4 s $^{-1}$ for wild-type, 0.023 s $^{-1}$ for R282A, and 0.010 s $^{-1}$ for R282K RhoGAPs (Figure 1). Thus, there is a 230- and 540-fold reduction in GAP activity caused by mutation of Arg-282 to alanine and lysine, respectively. With R282K RhoGAP, a hyperbolic dependence of k_{obs} on GAP concentration was seen with a K_m of 3.9 μM . Although the saturation curve was not well defined, with both wild-type and R282A RhoGAPs the K_m was <0.5 μM .

The rate constant of the intrinsic Rho-GTPase was determined to be 1.4×10^{-4} s $^{-1}$ (data not shown). Thus, wild-type RhoGAP activates 38000-fold, R282A 160-fold, and R282K 70-fold.

Measurement of the Affinity of Rho for Wild-Type, R282A, and R282K RhoGAP. First, the affinity of Rho-GMPPNP for wild-type, R282A, or R282K RhoGAPs was measured by isothermal titration calorimetry (ITC) (Figure 2). In each case, the binding was endothermic and the data could be fitted to a single-site binding isotherm. The measured stoichiometry of the interactions varied from 0.82 to 0.98. As it is known that 1 mol of Rho interacts with 1 mol of RhoGAP (6), the stoichiometries obtained indicate high

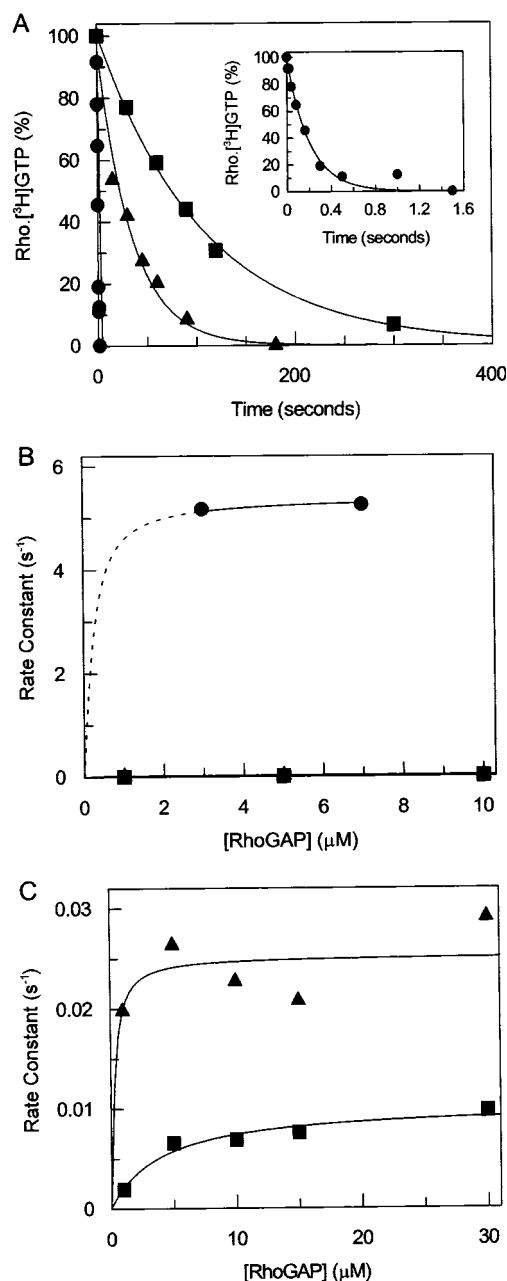


FIGURE 1: Single-turnover kinetic measurements of the catalytic parameters for wild-type, R282A, and R282K RhoGAPs. Various concentrations of wild-type (●), R282A (▲), or R282K (■) RhoGAPs were mixed with 0.2 μ M Rho \cdot [3 H]GTP. At intervals reactions in the samples were quenched by addition of perchloric acid, and the extent of hydrolysis was measured by HPLC. Mixing and quenching were performed in a quenched-flow apparatus (wild-type RhoGAP) or manually (mutant RhoGAPs). Time courses of hydrolysis were fitted to single exponentials. Panel A shows time points obtained with 7 μ M wild-type, 10 μ M R282A, and 10 μ M R282K RhoGAP. The solid lines are the best fits with rate constants of 5.2, 0.023, and 0.0069 s^{-1} , respectively. The inset shows the data with wild-type RhoGAP on an expanded time scale. The observed pseudo-first-order rate constants are plotted against concentration of RhoGAP (B and C). The curves shown are fits to single-binding site isotherms, with the following parameters: wild-type, $K_m = 0.2$ μ M and $k_{cat} = 5.4$ s^{-1} ; R282A, $K_m = 0.2$ μ M and $k_{cat} = 0.023$ s^{-1} ; and R282K, $K_m = 3.9$ μ M and $k_{cat} = 0.01$ s^{-1} . Panel C displays the data for mutant RhoGAPs on an expanded scale.

activity of the proteins, suggesting that the mutations had no gross effect on protein stability. The K_d values calculated

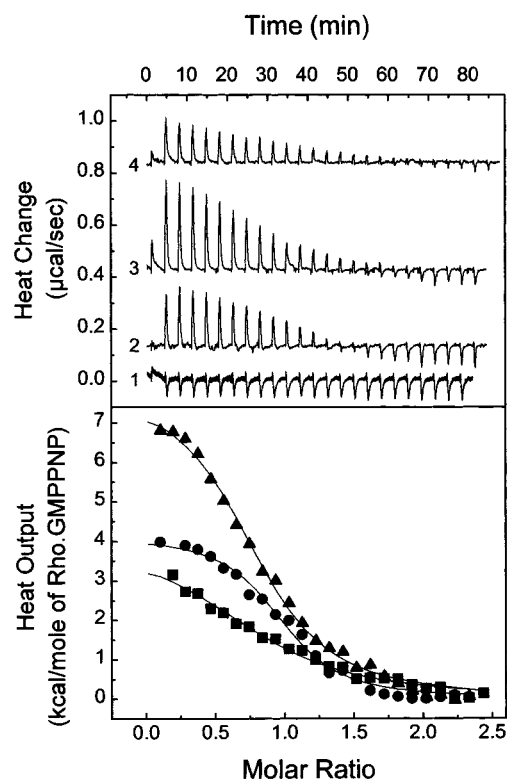


FIGURE 2: ITC measurements of the affinity of Rho \cdot GMPPNP for wild-type, R282A, and R282K RhoGAP. Rho \cdot GMPPNP (0.18 mM) was titrated into buffer alone (trace 1), 15 μ M wild-type RhoGAP (trace 2, ●), 15 μ M R282A RhoGAP (trace 3, ▲), or 15 μ M R282K RhoGAP (trace 4, ■) in an isothermal titration calorimeter, and heat changes were monitored continuously. The raw data from each injection are shown in the top panel. The measured heats from each peak were integrated, and the buffer control was subtracted from those with RhoGAP. The resultant data are plotted in the lower panel as the molar ratio of Rho \cdot GMPPNP injected to RhoGAP present against the heat output per mole of injected Rho \cdot GMPPNP. The lines through the points are the best fits to the data assuming a single binding site model with the following parameters: $K_d = 0.8$ μ M, $n = 0.98$, and $\Delta H = 4.1$ kcal mol $^{-1}$ for wild-type, $K_d = 1.6$ μ M, $n = 0.82$, and $\Delta H = 7.9$ kcal mol $^{-1}$ for R282A, and $K_d = 3.5$ μ M, $n = 0.86$, and $\Delta H = 4.1$ kcal mol $^{-1}$ for R282K RhoGAP.

for wild-type, R282A, and R282K RhoGAP were 0.8, 1.6, and 3.5 μ M, respectively. Thus, the substitution of lysine for arginine has resulted in an approximate 4-fold decrease, whereas the alanine substitution causes an only 2-fold decrease in binding affinity.

It has previously been observed that aluminum fluoride mediates the formation of a stable complex between RhoGAP and Rho \cdot GDP (6) or Cdc42 \cdot GDP (17, 27). We have investigated the contribution of the conserved Arg-282 residue in the formation of this complex. ITC experiments in the presence of AlF_x showed that titration of Rho \cdot GDP into wild-type or R282A RhoGAP was associated with a strongly endothermic heat change, which fitted well to a single-binding site isotherm (Figure 3) with a stoichiometry of 0.9–1.0. The K_d s for wild-type and R282A RhoGAP binding to Rho \cdot GDP with AlF_x were calculated as 0.4 and 0.9 μ M, respectively, showing that the arginine to alanine mutation resulted in an only 2-fold decrease in affinity. No heat changes were observed when Rho \cdot GDP was titrated into R282K RhoGAP in the presence of AlF_x ; hence, no conclusions regarding binding could be made.

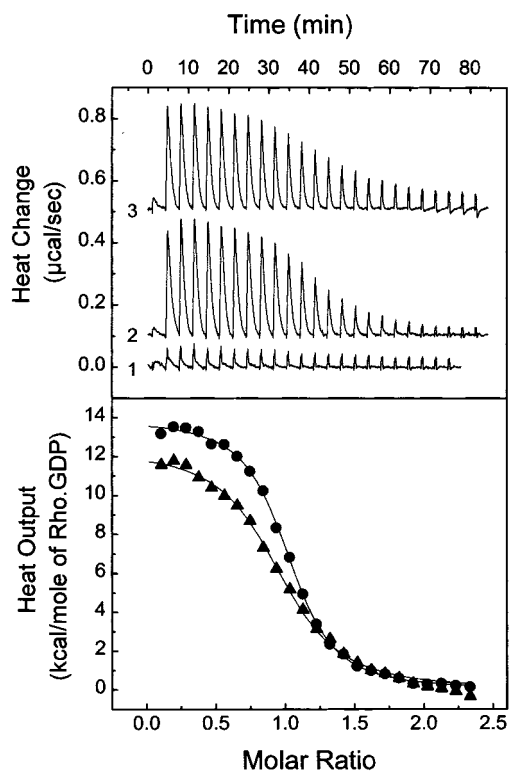


FIGURE 3: ITC measurements of the affinity of Rho•GDP for wild-type and R282A RhoGAP in the presence of AlF_x . Experiments were performed in the presence of $110 \mu\text{M}$ AlCl_3 and 20 mM NaF . Rho•GDP (0.18 mM) was titrated into buffer alone (trace 1), $15 \mu\text{M}$ wild-type RhoGAP (trace 2, ●), or $15 \mu\text{M}$ R282A RhoGAP (trace 3, ▲) in an isothermal titration calorimeter. The raw data from each injection are shown in the top panel. The measured heats from each peak were integrated, and the buffer control was subtracted from those with RhoGAP. The resultant data are plotted in the lower panel as the molar ratio of Rho•GDP injected to RhoGAP present against the heat output per mole of injected Rho•GDP. The lines through the points are the best fits to the data assuming a single binding site model with the following parameters: $K_d = 0.4 \mu\text{M}$, $n = 1.0$, and $\Delta H = 13.9 \text{ kcal mol}^{-1}$ for wild-type and $K_d = 0.9 \mu\text{M}$, $n = 0.9$, and $\Delta H = 12.5 \text{ kcal mol}^{-1}$ for R282A RhoGAP.

We verified the ITC binding data using an equilibrium binding assay which relied on a different type of measurement. Scintillation proximity assay (SPA) procedures, similar to those previously used to measure affinities of Ras–Raf (28), Ras–NF1 (22), Rac–PAK, and Cdc42–PAK (23) interactions, were utilized. The apparent K_d s obtained using SPA are similar to those obtained with true solution methods (23, 29). In these assays, a signal is obtained when either Q61L Rac• $[\text{}^3\text{H}]\text{GTP}$ or Q63L Rho• $[\text{}^3\text{H}]\text{GTP}$ binds to GST–RhoGAP linked to SPA beads. From experiments in which the concentration of Rho• $[\text{}^3\text{H}]\text{GTP}$ was varied, the apparent K_d s of Q63L Rho•GTP for wild-type, R282A, and R282K RhoGAPs were found to be 0.016 , 0.014 , and $0.3 \mu\text{M}$, respectively. Similar experiments with Q61L Rac•GTP gave apparent K_d s of 0.20 , 0.06 , and $1.6 \mu\text{M}$, respectively. Then, SPAs were performed in which Rho complexed with unradiolabeled nucleotides was titrated into assays with fixed concentrations of Q61L Rac• $[\text{}^3\text{H}]\text{GTP}$ and either wild-type or mutant RhoGAPs, thereby competing with radiolabeled Rac and causing a decrease in signal. Using this procedure, the apparent K_d s for Rho•GMPPNP binding to wild-type and R282A RhoGAP were found to be 2.3 and $5.7 \mu\text{M}$, respectively, supporting the conclusion obtained by ITC that

the mutation results in a small loss in affinity (Table 1). In the absence of AlF_x , binding of Rho•GDP to either wild-type or R282A RhoGAP was similar and weak ($K_d \geq 30 \mu\text{M}$) (Figure 4 and Table 1). In the presence of AlF_x , the apparent K_d s for Rho•GDP binding to wild-type and R282A RhoGAP were 1.1 and $3.7 \mu\text{M}$, respectively (Figure 4 and Table 1). These data confirmed that the alanine substitution only has a small effect on the ability of RhoGAP to form the Rho•GDP• AlF_x •RhoGAP complex.

Interaction between Wild-Type and Mutant RhoGAPs with Rho Complexed with mant Nucleotides. Hoffman et al. (17) reported that mutation of the conserved arginine resulted in a 50-fold loss of affinity for Cdc42•mantGDP in the presence of AlF_x , and hence concluded that this arginine was required for formation of the AlF_x -mediated complex. This contrasts with our data, using GDP itself showing an only 2–3-fold decrease in affinity (Table 1). Although we and others have found that mant nucleotides can behave as good analogues of GTP or GDP, the following experiments suggested that this discrepancy was related to the use of mantGDP rather than GDP. SPA experiments were performed to measure affinities for Rho•mantGDP in the presence of AlF_x . The K_d for wild-type RhoGAP binding to Rho•mantGDP was $1.9 \mu\text{M}$, similar to that for binding to Rho•GDP ($1.1 \mu\text{M}$) (Figure 4 and Table 1). However, using R282A RhoGAP, Rho•mantGDP bound extremely poorly ($K_d \geq 30 \mu\text{M}$), whereas we showed above that Rho•GDP binds with high affinity ($K_d = 3.7 \mu\text{M}$). We also used fluorescence anisotropy, the technique used in ref 17, and found that any change in anisotropy upon mixing R282A RhoGAP with Rho•mantGDP in the presence of AlF_x was barely detectable, whereas wild-type RhoGAP gave a hyperbolic increase in anisotropy with a K_d of $2.3 \mu\text{M}$ (data not shown). Therefore, we believe that, perhaps due to the precise steric constraints required for formation of the AlF_x -mediated complex, replacement of arginine with alanine interferes with formation of the Rho•mantGDP but not with formation of the Rho•GDP complex.

DISCUSSION

Single-enzyme turnover experiments have been used previously to measure k_{cat} values of RasGAP-catalyzed Ras•mantGTPase (9, 10, 20). Here, we have determined k_{cat} for catalysis of Rho-GTPase by wild-type RhoGAP to be 5.4 s^{-1} . This represents a 38000-fold stimulation over the intrinsic Rho•GTP hydrolysis rate ($1.4 \times 10^{-4} \text{ s}^{-1}$). This level of stimulation is similar to those seen with p120-GAP and neurofibromin on Ras•mantGTP (10, 20).

The k_{cat} for R282A RhoGAP was 0.023 s^{-1} and for R282K RhoGAP was 0.010 s^{-1} . These values represent a reduction in the ability of RhoGAP to stimulate Rho-GTPase by 230- and 540-fold, respectively, showing that neither alanine nor lysine could substitute for arginine and maintain efficient catalysis. Since substitution with the basic side chain of lysine severely impaired the catalytic activity of RhoGAP, specific properties of the arginine side chain must be required.

The K_m values of wild-type and mutant RhoGAPs for wild-type Rho•GTP were estimated from single-turnover kinetic experiments (Figure 1 and Table 1). If the initial binding step is a rapid equilibrium relative to k_{cat} , as has previously been assumed in measuring RasGAP kinetics (10, 26), K_m

Table 1: Catalytic and Equilibrium Dissociation Constants for Wild-Type and Mutant RhoGAP^a

Rho complex	method	wild-type RhoGAP		R282A RhoGAP		R282K RhoGAP	
		K_d (μ M)	k_{cat} (s^{-1})	K_d (μ M)	k_{cat} (s^{-1})	K_d (μ M)	k_{cat} (s^{-1})
Rho•GTP	GTPase	$\geq 0.5^b$	5.4	$\geq 0.5^b$	0.023	3.9 ^b	0.010
Rho•GMPPNP	ITC	0.8		1.6		3.5	
	SPA	2.3		5.7		^c	
Rho•GDP	SPA	≥ 30		≥ 30		^c	
Rho•GDP and AlF _x	ITC	0.4		0.9		^d	
	SPA	1.1		3.7		^c	
Rho•mantGDP and AlF _x	SPA	1.9		≥ 30		^c	
Q63L Rho•GTP	SPA	0.016		0.014		0.3	
Q61L Rac•GTP	SPA	0.2		0.06		1.6	

^a Catalytic and equilibrium dissociation constants were measured using the indicated methods as described in Experimental Procedures and in the legends of Figures 1–4. ^b K_m value ($\geq K_d$). ^c SPA signal insufficient to allow K_d determination. ^d No heat change seen.

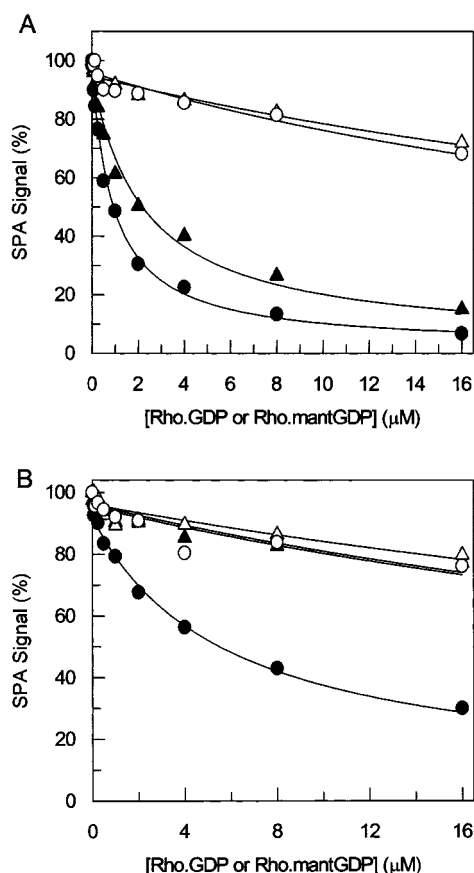


FIGURE 4: SPA measurements of Rho•GDP and Rho•mantGDP binding to wild-type and R282A RhoGAP in the presence and absence of aluminum fluoride. The indicated concentrations of Rho•GDP or Rho•mantGDP were added to SPAs containing Q61L Rac•[³H]GTP and either wild-type GST–RhoGAP (A) or R282A GST–RhoGAP (B), and the SPA signal was measured. The signal from a blank without GST–RhoGAP was subtracted, and the data were plotted as a percentage of the signal without added Rho•GDP or Rho•mantGDP. The solid lines represent the best fit to an equation describing competitive inhibition of binding of radiolabeled Rac to GST–RhoGAP. With wild-type RhoGAP, the apparent K_d values are 32 μ M for Rho•GDP without AlF_x (○) and 1.1 μ M with AlF_x (●) and 40 μ M for Rho•mantGDP without AlF_x (△) and 1.9 μ M with AlF_x (▲). With R282A RhoGAP, the apparent K_d values are 34 μ M for Rho•GDP without AlF_x (○) and 3.7 μ M with AlF_x (●) and 45 μ M for Rho•mantGDP without AlF_x (△) and 34 μ M with AlF_x (▲).

will equal K_d . In any case, the true K_d for interaction with Rho•GTP will be less than or equal to this measured K_m . The K_d s of RhoGAPs for Rho•GMPPNP and for Q63L Rho•GTP and Q61L Rac•GTP complexes, none of which show

significant hydrolysis during the time course of the experiments, were measured directly from ITC and SPA experiments (Table 1). These methods gave comparable values for K_d s, although the affinity measured by ITC was about 2–3-fold higher than that estimated by the SPA. The K_d for wild-type RhoGAP binding to Rho•GMPPNP reported here is similar to that previously published (30, 31). The alanine mutation resulted in a small decrease (2–3-fold) in the affinity of RhoGAP for Rho•GMPPNP and no measurable difference in the affinity for wild-type or Q63L Rho•GTP and actually increased its affinity for the GTP form of Q61L Rac (Table 1 and ref 14). The lysine mutation resulted in a more significant impairment of binding (≥ 4 -fold decrease) to both Rho and Q61L Rac (Table 1), suggesting a slightly greater structural perturbation than in the alanine mutation.

Thus, Arg-282 contributes 230-fold out of the total 38000-fold catalytic stimulation by RhoGAP but is not required for binding of RhoGAP to the triphosphate-bound conformation of Rho. This conclusion is in qualitative agreement with reported data on the role of the conserved arginine in n-chimaerin (13), myr5 (15), Cdc42GAP/RhoGAP (14, 17, 18), and p190GAP (16).

As R282A RhoGAP still increases the level of Rho•GTPase by 160-fold, we conclude that transition-state stabilization by Arg-282 contributes about 50% of the reduction in activation energy by RhoGAP and other factors account for the remaining half of its catalytic power. Similarly, RasGAP without the catalytic arginine stimulates Ras•GTPase by at least 100-fold (10). In both RhoGAP and RasGAPs, catalytic enhancement is likely to arise both from stabilization of a conformation most complementary to the transition state (6, 10, 32) and also from ground-state destabilization. The latter is supported by the observation of catalytically inactive RasGAP and n-chimaerin mutants which bind with increased affinity to the triphosphate forms of their respective G protein partners (13, 33).

In accordance with transition-state theory, there are groups on enzymes which interact better with the transition state than with the unaltered substrate (34, 35). The improvement in binding energy by going from the substrate to transition state lowers the activation energy of the reaction and so increases the catalytic rate. As discussed by Fersht (35), under conditions of saturating substrate, catalysis occurs when the binding energy is realized only in the transition-state complex; i.e., its energy is lowered while that of the enzyme–substrate complex remains the same. This lowers the activation energy of k_{cat} and so increases the rate of

reaction. Removal of a side chain which only binds the substrate in the transition state should therefore leave K_d for substrate binding unaltered and just lower k_{cat} (34). Removal of Arg-282 reduces k_{cat} by 230-fold, but with a negligible effect on substrate binding. The apparent binding energy for binding of the arginine side chain to the transition state is 3.2 kcal/mol, from the equation $\Delta G = -RT \ln(k_{cat}^{mutant}/k_{cat}^{wild-type})$ (34). Conversely, the R282A mutant RhoGAP should bind 230-fold weaker to the transition state. RhoGAPs and RasGAPs form AlF_x -mediated ternary complexes with the GDP forms of their respective small G protein partners, which have been proposed to represent analogues of the transition state of the Rho (or Ras)-GTPase reaction (6–8, 17, 27). Thus, if the complex precisely mimics the transition state, it was anticipated that the R282A RhoGAP would bind with a 230-fold reduced affinity for Rho•GDP in the presence of AlF_x . However, although AlF_x increased the affinity of binding of Rho•GDP to RhoGAP by more than 30-fold (Table 1), consistent with the formation of a complex closer to the transition state, we found that R282A RhoGAP also effectively forms the Rho•GDP• AlF_x •RhoGAP complex (Table 1). Thus, Arg-282 is not required for formation of this complex. This suggests that arginine is not fulfilling the same role in stabilizing the Rho•GDP• AlF_x •RhoGAP complex as it is predicted to do in the transition state.

Our data show that the affinity of wild-type RhoGAP for Rho•GDP in the presence of AlF_x is the same or lower than that for Rho•GTP and about 2-fold higher than that for Rho•GMPPNP (Table 1). We have concluded above that at least 230-fold of the catalytic rate enhancement is likely due to transition state stabilization, and hence, transition-state theory predicts that GAP would bind at least 230-fold tighter to the transition state than to the ground state of the substrate. Thus, also in this feature, the AlF_x complex does not have the anticipated properties of the transition state itself.

As we have found some features of the Rho•GDP• AlF_x •RhoGAP complex that are not expected of the transition state itself, it is appropriate to discuss the evidence which has been put forward to support G protein•GDP• AlF_x complexes being transition-state analogues. G_{α} •GDP was shown to be activated by both AlF_x and beryllium fluoride (36), and as both fluoride complexes were thought to be tetrahedrally coordinated, it was initially proposed that they acted as analogues of the γ -phosphate of GTP (37, 38). However, the X-ray structures of G_{α} •GDP• AlF_4^- revealed that the bound AlF_4^- was octahedrally coordinated with the fluorines present in a planar configuration (11, 12). This led to the proposal that the complex was a transition-state analogue, which was further supported by a structural rearrangement bringing the catalytic arginine into an appropriate conformation for catalysis (11, 12). Very likely, the structure is indeed close to a transition state, but for two reasons, this conclusion is not as clear as first thought. First, AlF_x in aqueous solution is not tetrahedral, but rather octahedral (39, 40). Thus, there might be no requirement for stabilization (e.g., by the catalytic arginine) of the AlF_4^- in the octahedral protein-bound form. Second, in G_{α} , mutation of the catalytic arginine showed that it is not absolutely required for AlF_x complex formation (11).

The structures of Ras•GDP• AlF_3 •RasGAP and Rho•GDP• AlF_4^- •RhoGAP complexes have many of the properties anticipated for the transition state (6, 8). They resemble the G_{α} structure in that the aluminum atom is coordinated by apical oxygens and by planar equatorial fluorines. Further, at least with RhoGAP, there is a conformational rearrangement versus the ground state with the movement of the catalytic arginine to form a close interaction with AlF_4^- (5, 6). However, it was clearly recognized (6) that the octahedral AlF_4^- configuration could only represent an approximation of the trigonal bipyramidal transition state. Mutation of the catalytic arginine of NF1 RasGAP either to lysine (9) or to alanine² effectively prevented formation of the AlF_x -mediated Ras•mantGDP or Ras•GDP complexes, respectively, as contrasted to an only 2–3-fold reduction in affinity when Arg-282 in the RhoGAP system is mutated. This may be due to the different coordinations of the aluminum between the Ras•GDP• AlF_3 •RhoGAP (8) and the Rho•GDP• AlF_4^- •RhoGAP complexes (6). In summary, the data reported here show that the major constituent of the Rho•GDP• AlF_x •RhoGAP complex in solution does not show the thermodynamic stabilization expected of the transition state, likely because of the different chemistry of the AlF_x complex and that of the true transition state, even though it might well be structurally a very close approximation.

ACKNOWLEDGMENT

We thank A. Hall for expression plasmids for RhoGAP and Rho, G. Thompson for purified Rac protein, S. Graham for mass spectrometry analysis, M. Goggin for large-scale fermentation, and R. Leatherbarrow and D. Trentham for critical evaluation of the manuscript.

REFERENCES

- Ridley, A. J. (1996) *Curr. Biol.* 6, 1256–1264.
- Ridley, A. J. (1997) *Biochem. Soc. Trans.* 25, 1005–1010.
- Lamarche, N., and Hall, A. (1994) *Trends Genet.* 10, 436–440.
- Lancaster, C. A., Taylor-Harris, P. M., Self, A. J., Brill, S., van Erp, H. E., and Hall, A. (1994) *J. Biol. Chem.* 269, 1137–1142.
- Rittinger, K., Walker, P. A., Eccleston, J. F., Nurmahomed, K., Owen, D., Laue, E., Gamblin, S. J., and Smerdon, S. J. (1997) *Nature* 388, 693–697.
- Rittinger, K., Walker, P. A., Eccleston, J. F., Smerdon, S. J., and Gamblin, S. J. (1997) *Nature* 389, 758–762.
- Mittal, R., Ahmadian, M. R., Goody, R. S., and Wittinghofer, A. (1996) *Science* 273, 115–117.
- Scheffzek, K., Ahmadian, M. R., Kabsch, W., Wiesmuller, L., Lautwein, A., Schmitz, F., and Wittinghofer, A. (1997) *Science* 277, 333–338.
- Ahmadian, M. R., Stege, P., Scheffzek, K., and Wittinghofer, A. (1997) *Nat. Struct. Biol.* 4, 686–689.
- Sermon, B. A., Lowe, P. N., Strom, M., and Eccleston, J. F. (1998) *J. Biol. Chem.* 273, 9480–9485.
- Coleman, D. E., Berghuis, A. M., Lee, E., Linder, M. E., Gilman, A. G., and Sprang, S. R. (1994) *Science* 265, 1405–1412.
- Sondek, J., Lambright, D. G., Noel, J. P., Hamm, H. E., and Sigler, P. B. (1994) *Nature* 372, 276–279.
- Ahmed, S., Lee, J., Wen, L. P., Zhao, Z. S., Ho, J., Best, A., Kozma, R., and Lim, L. (1994) *J. Biol. Chem.* 269, 17642–17648.
- Graham, D. L., Eccleston, J. F., and Lowe, P. N. (1997) *Biochem. Soc. Trans.* 25, 512S.
- Muller, R. T., Honnert, U., Reinhard, J., and Bahler, M. (1997) *Mol. Biol. Cell* 8, 2039–2053.

² P. N. Lowe, unpublished observations.

16. Li, R., Zhang, B. L., and Zheng, Y. (1997) *J. Biol. Chem.* 272, 32830–32835.
17. Hoffman, G. R., Nassar, N., Oswald, R. E., and Cerione, R. A. (1998) *J. Biol. Chem.* 273, 4392–4399.
18. Leonard, D. A., Lin, R., Cerione, R. A., and Manor, D. (1998) *J. Biol. Chem.* 273, 16210–16215.
19. Self, A. J., and Hall, A. (1995) *Methods Enzymol.* 256, 3–10.
20. Eccleston, J. F., Moore, K. J., Morgan, L., Skinner, R. H., and Lowe, P. N. (1993) *J. Biol. Chem.* 268, 27012–27019.
21. Mach, H., Middaugh, C. R., and Lewis, R. V. (1992) *Anal. Biochem.* 200, 74–80.
22. Skinner, R. H., Picardo, M., Gane, N. M., Cook, N. D., Morgan, L., Rowedder, J., and Lowe, P. N. (1994) *Anal. Biochem.* 223, 259–265.
23. Thompson, G., Owen, D., Chalk, P. A., and Lowe, P. N. (1998) *Biochemistry* 37, 7885–7891.
24. Jameson, D. M., and Eccleston, J. F. (1997) *Methods Enzymol.* 278, 363–390.
25. Wiseman, T., Williston, S., Brandts, J. F., and Lin, L. N. (1989) *Anal. Biochem.* 179, 131–137.
26. Ahmadian, M. R., Hoffmann, U., Goody, R. S., and Wittinghofer, A. (1997) *Biochemistry* 36, 4535–4541.
27. Ahmadian, M. R., Mittal, R., Hall, A., and Wittinghofer, A. (1997) *FEBS Lett.* 408, 315–318.
28. Gorman, C., Skinner, R. H., Skelly, J. V., Neidle, S., and Lowe, P. N. (1996) *J. Biol. Chem.* 271, 6713–6719.
29. Lawton, D. G., Gorman, C., and Lowe, P. N. (1997) *Biochem. Soc. Trans.* 25, 510S.
30. Self, A. J., and Hall, A. (1995) *Methods Enzymol.* 256, 67–76.
31. Zhang, B., Chernoff, J., and Zheng, Y. (1998) *J. Biol. Chem.* 273, 8776–8782.
32. Sprang, S. R. (1997) *Science* 277, 329–330.
33. Morcos, P., Thapar, N., Tusneem, N., Stacey, D., and Tamanoi, F. (1996) *Mol. Cell. Biol.* 16, 2496–2503.
34. Wells, N. C., and Fersht, A. R. (1985) *Nature* 316, 656–657.
35. Fersht, A. (1984) in *Enzyme Structure and Mechanism*, 2nd ed., pp 311–346, W. H. Freeman & Co., New York.
36. Sternweis, P. C., and Gilman, A. G. (1982) *Proc. Natl. Acad. Sci. U.S.A.* 79, 4888–4891.
37. Bigay, J., Deterre, P., Pfister, C., and Chabre, M. (1985) *FEBS Lett.* 191, 181–185.
38. Bigay, J., Deterre, P., Pfister, C., and Chabre, M. (1987) *EMBO J.* 6, 2907–2913.
39. Akitt, J. W. (1989) *Prog. Nucl. Magn. Reson. Spectrosc.* 21, 1–150.
40. Martinez, E. J., Girardet, J. L., and Morat, C. (1996) *Inorg. Chem.* 35, 706–710.

BI9821770